Check for updates

The bleaching limits of IRSL signals at various stimulation temperatures and their potential inference of the pre-burial light exposure duration

Jingran Zhang[1]*, Benny Guralnik[2†], Sumiko Tsukamoto[3], Christina Ankjærgaard[4] and Tony Reimann[5]

[1]School of Geography, Nanjing Normal University, Key Laboratory of Virtual Geographic Environment, Ministry of Education of China, Jiangsu Open Laboratory of Major Scientific Instrument and Equipment, Nanjing, China, [2]Technical University of Denmark, Kongens Lyngby, Denmark, [3]Leibniz Institute for Applied Geophysics, Hannover, Germany, [4]Department of Health Technology, Technical University of Denmark, Roskilde, Denmark, [5]Institute of Geography, University of Cologne, Cologne, Germany

Infrared Stimulated Luminescence (IRSL) techniques are being increasingly used for dating sedimentary feldspars in the middle to late Quaternary. By employing several subsequent stimulations at increasing temperatures, a series of post-IR IRSL (pIRIR) signals with different characteristics (stability and bleachability) can be obtained for an individual sample. It has been experimentally demonstrated that higher-temperature pIRIR signals are more stable, but they tend to exhibit larger residual doses up to few tens of Gy, potentially causing severe age overestimation in young samples. In this study we conducted comprehensive bleaching experiments of IRSL and pIRIR signals using a loess sample from China, and demonstrated that non-bleachable components in the IR (and possibly pIRIR) signals do exist. The level of such non-bleachable signal shows clearly positive correlation with preheat/stimulation temperature, which further supports the notion that lower temperature pIRIR are advantageous to date young samples and sediments especially from difficult-to-bleach environments. These results display a potential in constrain the pre-burial light exposure history of sediment utilizing multiple feldspar post-IR IRSL (pIRIR) signals. For the studied loess sample, we infer that prior to its last burial, the sample has received an equivalent of >264 h exposure to the SOL2 simulator (more than 2,000 h of natural daylight).

Introduction

Luminescence dating is a widely established Quaternary dating method, which is typically used to quantify the amount of time elapsed since a sediment has been last exposed to sunlight (Rhodes, 2011). The method is based on interpolating the natural luminescence intensity onto a regenerated dose response in the laboratory, producing an equivalent dose (D_e) which is the dose the sample has received in nature. The post-IR IRSL (pIRIR) technique, including the two-step pIRIR (Thomsen et al., 2008; Thiel et al., 2011) and multi-elevated-temperature (MET) pIRIR (Li and Li, 2011; Fu and Li, 2013), has been developed based upon the conventional IRSL for dating various sedimentary feldspars. The stability and bleachability are two crucial properties of any luminescence signal to be used for reliable dating, and in the case of feldspar IRSL or pIRIR seem to be interrelated (Jain et al., 2012). The fading rate of pIRIR signals generally decreases with higher stimulation temperature (e.g., Thomsen et al., 2008; Thiel et al., 2011; Li and Li, 2011; Buylaert et al., 2012), however the more stable signals are also progressively difficult to bleach (e.g., Li and Li, 2011; Kars et al., 2014a; Colarossi et al., 2015). As a result, pIRIR signals may be unaffected by anomalous fading but raise concerns about potential age overestimation caused by the unbleachable component (residual), especially for young samples.

So far, the origin and underlying mechanism of this residual signal is still poorly understood. The bleachability and the subsequent residual dose of pIRIR signals has drawn intensive discussions about its effect on a reliable dose determination and whether it should be subtracted. In some cases, modern analogues or artificially bleached samples have also been employed to check the bleachability and any residual dose subtraction (e.g., Buylaert et al., 2011; Li and Li, 2011; Reimann et al., 2011; Fu et al., 2012). Buylaert et al. (2012) proposed a sample-independent characteristic residual of ~4 ± 2 Gy for the pIRIR signal measured at 290°C (pIRIR$_{290}$), as obtained from a finite intercept extrapolated from a group of samples with different burial doses. A commonly agreed opinion is that residual doses might be negligible for older samples but could cause severe age overestimation for young samples. Interestingly, Sohbati et al. (2012) and Zhang et al. (2015a) reported no significant unbleachable residual dose (<10 Gy) in both IR$_{50}$ and pIRIR$_{225}$ signals (after 4 h of SOL2 bleaching), although a positive correlation between the residual doses and the natural doses was noticed. Consequently, no residual correction has been applied for their ages. Conversely, Buylaert et al. (2013) observed no significant trend of residual doses (due to 4 h SOL2) against their corresponding natural doses, and adopted a mean residual dose of 12.6 ± 0.7 Gy to be subtracted from all natural D_es. This difficult-to-bleach component of the pIRIR signal has been considered arising from thermal transfer (Buylaert et al., 2012, 2013). Kars et al. (2014a) carried out comprehensive bleaching experiments for

feldspar by exposing samples in the solar simulator with a series of exposure time from 1 h to 11 days. They demonstrated that pIRIR signals measured at higher temperatures are increasingly harder to bleach but none of their bleaching curves reach a plateau within 11 days of solar simulator exposure. Later on, Colarossi et al. (2015) argued that there may be no unbleachable component of pIRIR signal based on the fact that both IR$_{50}$ and pIRIR signals derived from pIRIR$_{225}$ and pIRIR$_{290}$ protocols display a monotonic decrease and do not reach a stable unbleachable limit within 14 days of solar simulator exposure, similar to that of Kars et al. (2014a). However, it is noteworthy that there is still a considerable amount of signal remaining even after 14 days exposure to the solar simulator especially for higher stimulation temperature (e.g., pIRIR$_{290}$) in both studies. Furthermore, Kars et al. (2014a) demonstrated a tendency that the pIRIR signal of young samples bleached much slower than that of the older samples. Yi et al. (2016, 2018) carried out prolonged bleaching experiments (>80 days in solar simulator) for pIRIR$_{290}$ of loess samples from northeastern and southeastern China. The pIRIR$_{290}$ residual signals reached a plateau after ~300 h exposure in both studies, and a constant residual corresponding to a dose of 4–6 Gy were observed. More recently, Cheng et al. (2022) investigated the bleachability of the single grain K-feldspar pIRIR signals and observed significant variations in residual doses (ranging from ~1 Gy to up to ~37 Gy after 40 h sunlight bleaching) among different grains from the same sample, that could cause additional scatter in D_e values.

Due to their differential bleaching rates, the comparison of feldspar IRSL and pIRIR ages with quartz OSL ages can be used to identify well bleached quartz (Murray et al., 2012), and even qualitatively determine the degree of bleaching (Reimann et al., 2015) helping to infer the transport history of various sediments. The development of rock surface exposure dating has allowed to quantify the amount of time that a rock surface has been exposed to sunlight, via utilizing the spatiotemporal evolution of the luminescence bleaching front within a solid (Sohbati, 2013). However, the exposure time of sediments to sunlight prior to their deposition is a relatively unexplored area (Reimann et al., 2015) where assumptions and speculations often dominate. The length of a sediment's exposure to sunlight prior to its deposition is important especially in young samples, where incomplete signal bleaching has the greatest effect on the age of the sediment (resulting in age overestimation). Very often, "modern analogues" (e.g., sediment from a nearby active channel) are used to quantify the expected "residual dose" in the sample of interest (e.g., Buylaert et al., 2009; Reimann et al., 2012; Li et al., 2014); however, such an estimation is valid only if both the modern sediment and the sample of interest experienced the same depositional environments, which is often questionable. Another existing approach is to administer a laboratory bleach for an arbitrary amount of time, and assume that it resets the signal to the level that it experienced in nature (reviewed in Li et al., 2014). Nevertheless, the degree of sediment bleaching prior

TABLE 1 Modified SAR protocol for pIRIR measurements.

Step	Measurement	Observation	Remark
1	Give dose, D_i (i=0, 1, 2, 3...)		
2	Preheat for 60 s @ 180–340°C with 20°C interval		
3	IR stimulation, 120 s at 50°C	L_x	IR_{50}
4	IR stimulation for 240 s @ 30°C below preheat in Step 2	L_x	pIRIR
5	Given dose, D_T (~1.72 Gy)		
6	Preheat for 60 s, @180–340°C with 20°C interval		
7	IR stimulation, 120 s @ 50°C	T_x	IR_{50}
8	IR stimulation, 240 s @ 30°C below preheat in Step 2	T_x	pIRIR
9	Return to step 1		

to deposition often remains unknown, and requires further investigation to prevent biased chronologies.

In this study, we measure multiple feldspar IR_{50} and pIRIR signals, and quantify their bleaching rates in the laboratory using SOL2. Through knowledge of an independent age of the same sample, we estimate pIRIR residual doses, and interpolate them onto a laboratory bleaching curve to obtain what we define as the equivalent bleaching time, B_e. This measure then allows us to infer the pre-burial light exposure duration.

Materials and methods

One young loess sample (LUM-2941) from China was chosen to explore the bleaching limit of its IRSL signals (both IR_{50} and pIRIR) at various thermal treatment conditions. It was collected from the northern piedmont of the Qilian Mountain, northwestern China (Zhang et al., 2015a; 2015b), and has been dated using both quartz and polymineral fine grains. The quartz OSL dating yielded an age of 6.3 ± 0.4 ka (Zhang et al., 2015b). The corresponding feldspar fading-corrected ages ranged between 5.8 ± 0.1 ka for $pIRIR_{150}$ and 7.2 ± 0.1 ka for $pIRIR_{310}$ (Zhang et al., 2015a). The dose rates for quartz and feldspar age calculation are 4.31 ± 0.25 Gy/ka and 4.89 ± 0.26 Gy/ka, respectively.

In this study, 14 groups of subsamples (27 aliquots in each group) were bleached in a Hönle SOL2 solar simulator using the full spectrum light, with exposure time ranging between 1 min and 20 days. An extra group of subsamples was prepared without SOL2 bleaching to obtain the natural signal as a reference. All measurements were carried out with an automated Risø DA-15 TL/OSL reader equipped with $^{90}Sr/^{90}Y$ beta source. The feldspar signal of the samples was stimulated with an array of infrared light diodes emitting at 870 nm, and the luminescence was detected through a filter combination of Schott BG39 and Corning 7–59 in the blue-violet region. Modified single-aliquot regenerative dose (SAR) protocols described in Zhang et al. (2015a) were applied; the preheat temperatures varied

between 180 and 340°C with 20°C interval and the second stimulation temperature was always 30°C lower than the preheat temperature (Table 1). The test dose was 1.72 Gy. Each data point is the average result of 3 aliquots.

Since the IRSL of feldspar is based on the localized recombination of electrons to nearest neighbour holes, it is expected that the IR_{50} and pIRIR bleaching curves follow power law decay (e.g., Jain et al., 2012). Therefore all bleaching curves were fitted with

$$I = At^{-b} + c \tag{1}$$

where I is normalized luminescence intensity after bleaching, A is a constant, t is the time, b is bleaching rate, and c is residual signal intensity.

Taking the independent age constraint of quartz OSL (6.3 ± 0.4 ka) as the true depositional age, the expected D_e of 30.8 ± 2.6 Gy was obtained for the sample. The fading corrected D_es of the sample were calculated based on the fading corrected feldspar ages (Zhang et al., 2015a) using the R 'Luminescence'-package (Dietze et al., 2013) according to the method of Huntley and Lamothe (2001). The difference between the fading-corrected D_es and the expected D_e (Table 2) was termed "predicted residual dose", and evaluated against the optical bleaching data using a reduced chi-square statistic (Bevington and Robinson, 2003).

Bleaching characteristics of feldspar IRSL signals

The luminescence intensity (L_n/T_n) of the IR_{50} (Figure 1A) and the pIRIR signals (Figure 1B) from all bleached subsamples was normalized to that of the natural subsamples (without bleaching) and plotted against SOL2 exposure time on a log-log scale. It is noteworthy that there is a kink exhibited for all bleaching curves at 1 hour exposure time, especially for pIRIR signals. It is because a new lamp in the solar simulator was used for the first five data points, referring to 1, 3, 5 min 10 and 20 min

TABLE 2 The measured IR$_{50}$ and pIRIR D$_e$s, g-values and the "predicted residual dose" (fading-corrected D$_e$ minus expected D$_e$) at various temperatures. The measured D$_e$s were previously presented in Zhang et al. (2015a). The expected D$_e$ of 30.8 ± 2.5 Gy is calculated from the quartz OSL age of 6.3 ± 0.4 ka (Zhang et al., 2015b).

Preheat temperature (°C)	Measured D$_e$ (Gy)		g-value (%/decade)		Fading-corrected D$_e$ (Gy)		Predicted residual dose (Gy)	
	IR$_{50}$	pIRIR	IR$_{50}$	pIRIR	IR$_{50}$	pIRIR	IR$_{50}$	pIRIR
180	21.9 ± 0.2	25.7 ± 0.2	2.84 ± 0.12	1.14 ± 0.22	28.5 ± 3.4	28.2 ± 1.6	-2.3 ± 4.3	-2.6 ± 3.0
200	23.3 ± 0.1	26.8 ± 0.1	2.90 ± 0.15	1.15 ± 0.03	30.3 ± 2.2	29.5 ± 1.6	-0.6 ± 3.4	-1.4 ± 3.0
220	25.0 ± 0.2	28.9 ± 0.2	2.56 ± 0.09	1.34 ± 0.40	31.7 ± 2.6	32.5 ± 2.1	0.9 ± 3.7	1.6 ± 3.3
240	26.6 ± 0.3	30.9 ± 0.2	2.45 ± 0.20	1.17 ± 0.25	33.3 ± 4.2	34.3 ± 2.0	2.4 ± 4.9	3.5 ± 3.2
260	27.8 ± 0.6	31.6 ± 0.8	2.06 ± 0.21	0.98 ± 0.15	33.5 ± 2.0	34.3 ± 2.1	2.7 ± 3.3	3.5 ± 3.3
280	25.9 ± 0.3	30.6 ± 0.1	1.69 ± 0.35	0.86 ± 0.34	30.1 ± 2.0	32.9 ± 1.9	-0.8 ± 3.2	2.1 ± 3.2
300	24.2 ± 0.2	31.7 ± 0.4	1.33 ± 0.15	0.75 ± 0.15	27.2 ± 1.5	33.7 ± 1.9	-3.7 ± 3.0	2.8 ± 3.2
320	23.9 ± 0.9	33.5 ± 0.3	1.07 ± 0.21	0.52 ± 0.34	26.3 ± 1.7	34.9 ± 2.1	-4.6 ± 3.1	4.0 ± 3.3
340	22.4 ± 0.8	35.5 ± 0.6	0.40 ± 1.02	-0.29 ± 0.73	23.1 ± 2.4	35.5 ± 0.6	-7.8 ± 3.5	4.6 ± 2.6

FIGURE 1
Normalized IR$_{50}$ **(A)** and pIRIR **(B)** luminescence intensity under various preheat (stimulation) temperatures, plotted against SOL2 bleaching time. The pIRIR stimulation temperature is always 30°C below the preheat temperature. The bleaching curves were fitted with the Eq. 1.
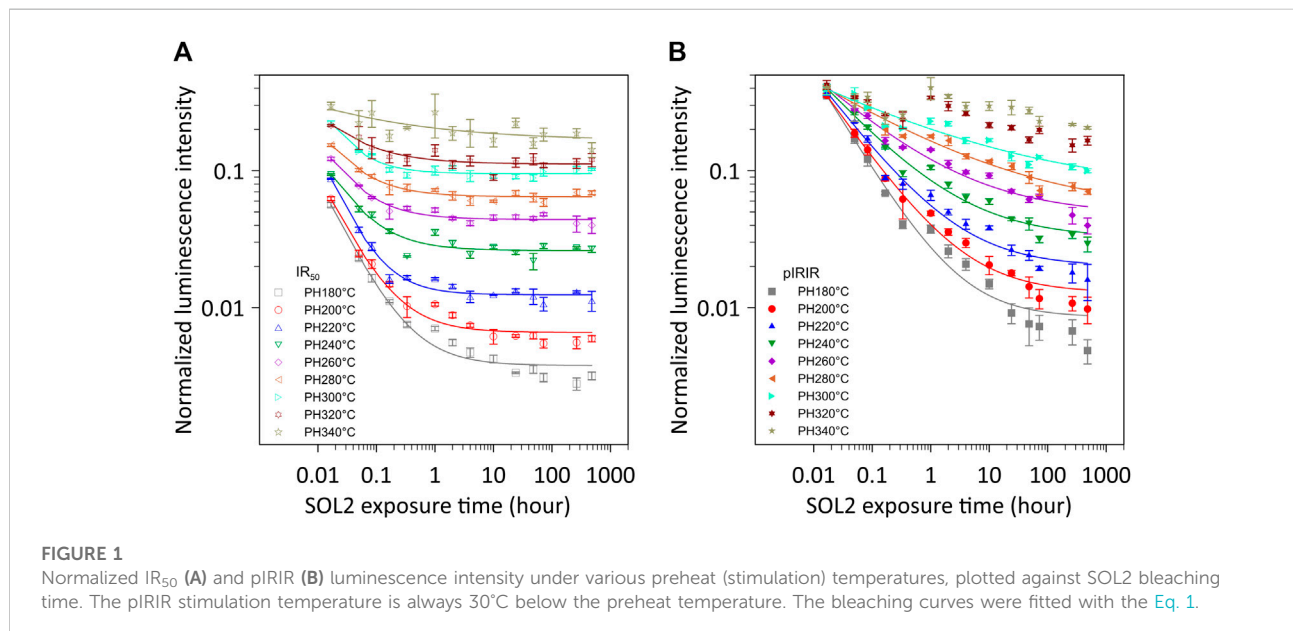
exposure time, as they were not included in the initial design of the experiment. Nevertheless, the general trend of these bleaching curves is not affected. As expected, the pIRIR signals bleach noticeably slower than their corresponding IR$_{50}$ signals, which is in line with previous studies. As shown in Figure 1, after 1 min (0.017 h) bleaching, the remaining IR$_{50}$ signals accounted for 6% of its natural signal intensity for the lowest temperature to up to 30% for the highest temperature, while all pIRIR signals are reduced to ~35–40%, with a similar trend like the IR$_{50}$ signals. The majority of the IR$_{50}$ bleaching data shows a noticeably nonlinear trend on a log-log scale,

asymptoting to a bleaching plateau after ~10 h exposure with seemingly unbleachable signals of up to 14% of their initial intensity (e.g. preheat at 340°C). Conversely, the pIRIR bleaching data do not appear to reach a steady-state level after 480 h exposure in SOL2 solar simulator. These findings are in line with Kars et al. (2014a) and Colarossi et al. (2015).

The bleaching curves were fitted to Eq. 1 given above. The fitted decay rate (*b*) and relative residual intensity (*c*) normalized to the natural signal are plotted in Figure 2. It was difficult to accurately fit the decay rate for the IR$_{50}$ signals, because the majority of the signals were bleached before 1 min (0.017 h)

FIGURE 2
(A) The fitted decay rate of pIRIR signals, and **(B)** relative residual intensity normalized to the natural signal for both IR_{50} and pIRIR signals.
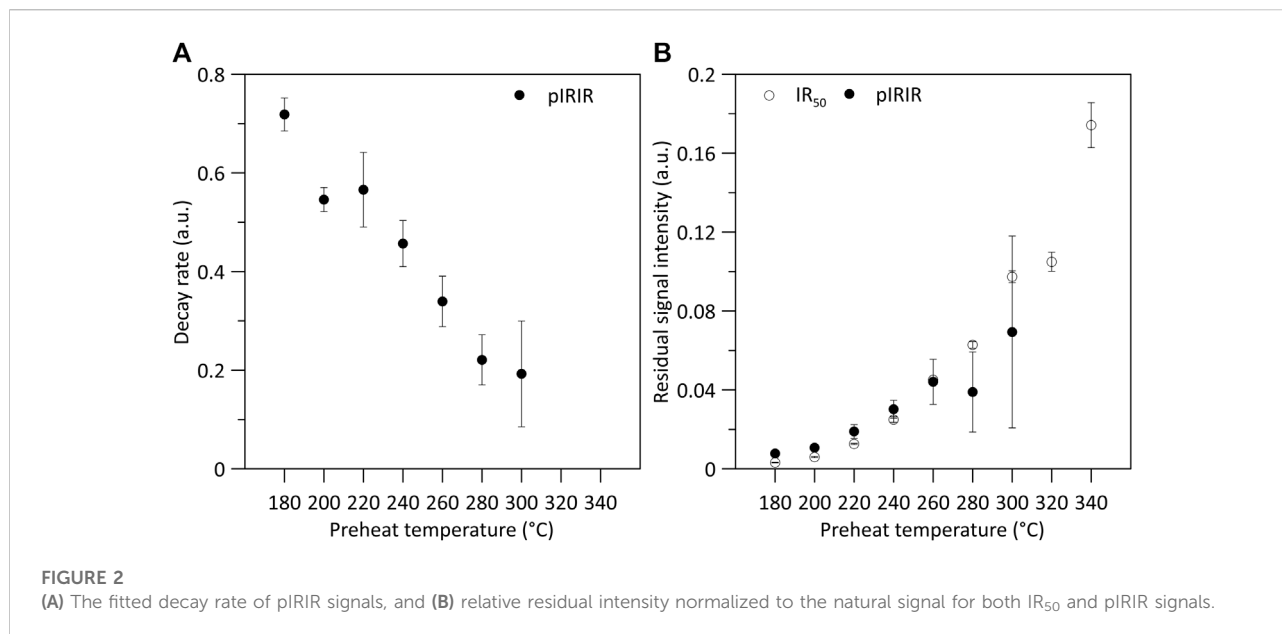
SOL2 exposure. The decay rate for the pIRIR signals shows a clear decreasing trend with increasing preheat (and stimulation) temperature (Figure 2A). The pIRIR bleaching curve for the two highest preheat temperatures could not be fitted to due to the scatter of the data. Nevertheless, Figure 2B indicates that the relative residual signal level, which increases with preheat temperature, is consistent between the IR_{50} and pIRIR signals for a same preheat temperature.

The preheat temperature dependence of the feldspar bleaching rate is in accordance with other studies (e.g., Li and Li, 2011; Lowick et al., 2012; Kars et al., 2014a; Colarossi et al., 2015; Reimann et al., 2015), and may be a result of increased distance between traps and recombination centres (e.g., Kars et al., 2014a). For both IR_{50} and pIRIR, more signal remains as the preheat temperature is raised (Figures 1A,B). The bleaching curve of IR_{50} after a 340°C preheat shows almost no clear decrease regardless of the exposure time. This may infer that the light-sensitive charges remaining after the SOL2 exposure have been further thermally removed during the high preheat and most of the detected signals might be originated from the thermal transfer of charge from light-insensitive traps to the IR-sensitive trap (Buylaert et al., 2011). The higher the temperature, the more charges could be thermally transferred. However, this does not explain the plateau at lower preheat temperatures (e.g.<200°C), at which thermal transfer should be minimal. An alternative explanation for the bleaching plateau may involve a competition between optical bleaching of the IR sensitive traps by SOL2, and repopulation of the same traps due to the UV component of the bleaching light (Ollerhead and Huntley, 2011). The equilibrium between optical de-trapping and UV trap refilling could be expected after prolonged exposure,

resulting in constant trap concentrations and hence bleaching curve plateaus. However, this hypothesis can also be questioned, as it cannot explain the presence of a plateau in one young coastal sample (W-Zi2; 0.84 ka) from Kars et al. (2014a), which was optically bleached with the UV part of the spectrum filtered out.

Based on the above observations, we confirm the presence of a non-bleachable component in the IRSL signal, and the high likelihood of the same phenomenon occurring in the pIRIR signal, and their strong correlation with preheat (stimulation) temperature. In order to minimize the effect of the residual signal on age determination, our results provide additional experimental evidence, and further support the notion that young samples should preferably be dated using lower preheat and stimulation temperatures in the pIRIR measurement protocol (Madsen et al., 2011; Reimann et al., 2011; Reimann and Tsukamoto, 2012; Zhang et al., 2015a; Reimann et al., 2015) or using the pulsed IR_{50} signal (Tsukamoto et al., 2017).

Inference of the pre-burial light exposure duration utilizing multiple feldspar pIRIR signals

The raw (i.e. fading uncorrected) measured D_e values of the IR_{50} and pIRIR signals of sample LUM-2941 (Zhang et al., 2015a) are shown as triangles in Figure 3. Alongside these direct measurements, the corresponding fading corrected D_e values are shown as squares. Up to 260°C, both IR_{50} and pIRIR datasets are generally in agreement, showing an increase in D_e values as a function of preheat temperature; above 260°C, the pIRIR D_es continue to increase, while the IR_{50} D_es reverse the
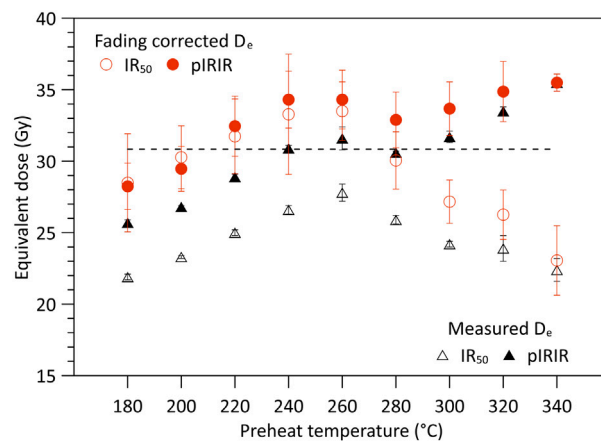
FIGURE 3
D_e values measured in the laboratory (triangles) and fading corrected D_es according to Zhang et al. (2015a). The dashed line denotes the expected D_e calculated based on the quartz OSL age. The pIRIR$_{310}$ D_e (preheat at 340°C) was not corrected as negative g-value was measured. The difference between the expected D_e and the fading corrected D_es is termed "predicted residual dose", and is further shown in Figure 4.
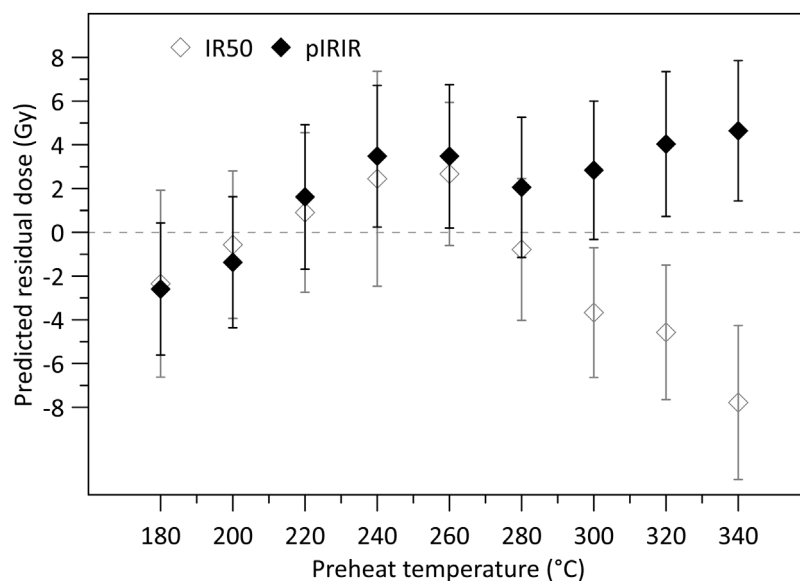
FIGURE 4
Predicted residual doses of the sample, corresponding to the differences between the fading-corrected D_es and the expected D_e (30.8 ± 2.6Gy). The detailed data were presented in Table 2.

trend and decrease, resulting in a peak D_e at a preheat of 260°C. The peak shape discloses an expectable artefact at preheat temperatures >260°C, which has been demonstrated by the failed dose recovery test of this sample (Figure 4A in Zhang et al. (2015a)) at the preheat temperatures >260°C. This behaviour of the IR$_{50}$ signals may be explained by trapping sensitivity change (Kars et al., 2014b). In the complete

absence of residual doses, the fading corrected D_es should have been the same as the expected D_e, given that the fading rate measurements and the applied model are both adequate. However, the fading corrected D_es of both IR$_{50}$ and pIRIR signals deviated from the expected value, and displayed a similar trend as the measured ones. As expected, the predicted residual dose increased with preheat temperature, up to 4.6 Gy (Figure 4). This
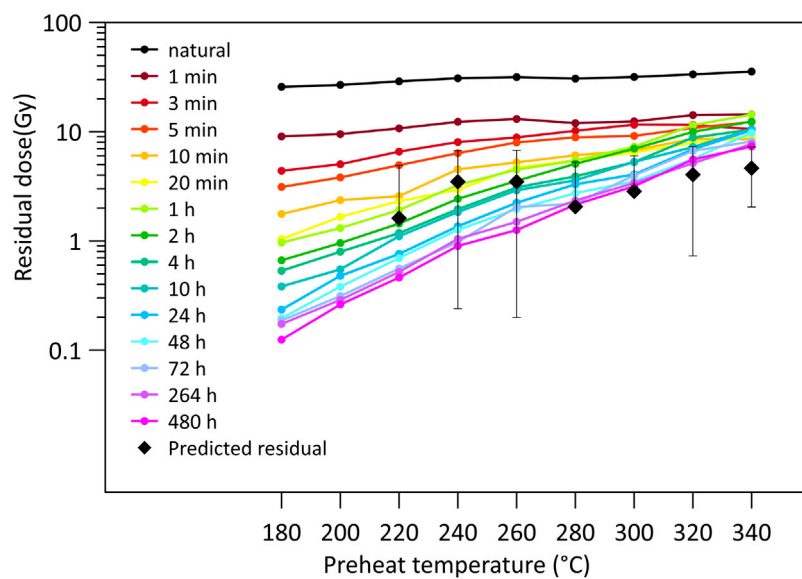
FIGURE 5
Predicted residual doses (solid diamonds; cf. Figure 4) superimposed onto the calculated residual doses from the laboratory bleaching experiments. The calculated residual doses refer to the remaining doses after different exposure times in SOL2. The uncertainties of the predicted residual doses were larger than the values themselves at preheat of 220, 280 and 300°C, so that the error bars on the negative direction cannot display on the log scale.

is in line with our observations in Figure 1, that the bleachability of feldspar pIRIR signals deteriorates towards higher measurement temperatures; consequently, higher residual doses for higher preheats may be expected, regardless of whether the sample is well or poorly bleached. It is noteworthy that for both IR_{50} and pIRIR signals, negative predicted residual doses were generated, which is unrealistic. One possible cause for negative residual doses is the uncertainty on the quartz OSL age (6.3 ± 0.4 ka); if the youngest age of 5.9 ka would be adopted, the negative values of the predicted residual doses would disappear. Another contributing factor is the well-documented trapping sensitivity change of the IR_{50} signal at preheat temperatures >260°C (Kars et al., 2014b), which makes the IR_{50} data not comparable across the different temperature. In the remainder of the paper, we therefore focus only on the pIRIR signal, which is also of primary interest for dating applications.

Since the dose response of the young sample is in its initial linear range, one can multiply the L_n/T_n depletion ratio of the bleaching experiments by the corresponding D_e of that pIRIR signal to obtain the remaining doses after different exposure times in SOL2. These are termed as "calculated residual dose", and are plotted against the corresponding preheat temperature in Figure 5. Predicted residual doses (solid black diamond; cf. Figure 4) were superimposed onto the calculated residual doses for comparison. Figure 5 shows that
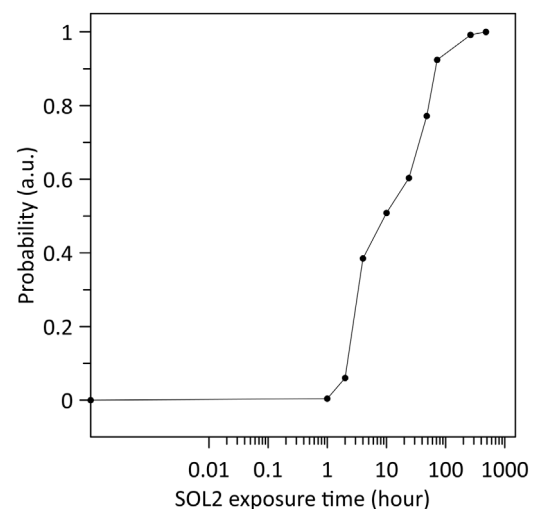
FIGURE 6
Probability of bleaching time prior to sedimentation, obtained by evaluating the goodness-of-fit of the predicted dose residuals against those from known bleaching times in Figure 5, using the reduced chi-square statistic.

the light exposure that this sample experienced prior to burial is probably longer than an equivalent of 4 h exposure in solar simulator that usually applied in residual test.

To estimate the probability of the bleaching time in nature prior to burial (Figure 6), we evaluated the goodness-of-fit of the predicted residual doses (black diamond in Figure 5) against observed residuals due to known bleaching times in the laboratory (coloured curves in Figure 5), using the reduced chi-square statistic. This enables us to translate the residual dose from the multiple luminescence signals into a B_e value that the sample has likely experienced before its last depositional event. We treated the standardized difference between the observed and predicted residual doses at each of the nine temperatures as a random variable following a standard normal distribution. In this case the sum of squares of these differences will be itself a random variable following a Chi-square distribution with nine degrees of freedom. The bleaching degree is calculated as the integrated area under the upper tail of the probability density curve of the Chi-square distribution, that is, the larger the Chi-square random variable (i.e., the larger the sum of squares of the differences), the smaller the integrated area within the upper tail of the distribution and therefore the lower the degree of bleaching. When all 14 data points of various bleaching time were included, the probability (i.e., the degree of bleaching) showed an early peak at a bleaching time of 20 min (Supplementary Figure S1). We argued that the appearance of this peak is unrealistic for the following reason. As mentioned above, the bleaching results of the first five data points (i.e., with exposure times of 1, 3, 5, 10, and 20 min) were measured using a new lamp, that is, different from the remaining data points (i.e., the exposure times of 1, 2, 4, ..., 480 h). As a consequence, a merger of the two sets of data will yield unexpected results. Accordingly, we excluded these five data point from Figure 6. We demonstrated that, for sample LUM-2941 collected from the northern piedmont of Qilian Mountains, when the laboratory exposure time exceeds 264 h, the corresponding bleaching degree is >95%. Since the intensity of SOL2 solar simulator is up to 9 times greater than daylight (Dr Honle Sol Sun simulation systems from Uvalight Technology Ltd, 1988), it means that this sample may experience more than two thousand hours daylight exposure prior to last burial in nature. This result implies that the use of standard residual subtraction (measured typically after 2–4 h bleach in SOL2; see Li et al., 2014) could lead to marked overestimation of the actual residual dose (264 h as in this study), leading to age underestimation which should be avoided.

According to the grain size analysis and process-related end-member (EM) modelling, Nottebaum et al. (2015) demonstrated that the dominant grain size fraction of the loess sample (LUM-2941) is coarse to fine silt fraction, which was classified as EM2 and EM3 population. The origin of EM2 and EM3 has been identified to be suspension during dust storm events from sandy and/or Gobi deserts surfaces located to the north of the Qilian Mountains, and constant long distance transport by westerlies, respectively. Both provenances are distant (>10^2 km) from the sampling locality. Regarding the possible travelling time during dust storms and trapping time before burial for such material, our reconstruction result, more than two thousand hours daylight exposure, is a plausible value, even though there is currently no other measure to validate or disprove it. Meanwhile, we are aware that our reconstruction is highly dependent on the availability of reliable age control, correct dose rate determination and accurate g-value measurements. Furthermore, the real sedimentological (transportation) process is rather complex, even for subaerial aeolian sedimentation. Such reconstruction of the B_e value simplifies the nature process, during which the daylight exposure is dominant. And it is noteworthy that such interpretation is only an attempt and the value of B_e is subject to slight difference in the way of calculation. At this stage of practice, the erosion-deposition cycles that the sediment may have experienced prior to the last exposure event have not been taken into consideration. Provided a sample had initially larger dose than the sample in this study (~30 Gy), longer bleaching time would be required to bleach the signals down to the same level.

The bleaching experiments presented in this paper were significantly time-consuming, because a range of pIRIR signals was explored and exploited for the interpolation of predicted residuals onto the laboratory bleaching curves. The advantage of using multiple pIRIR signals to obtain the natural bleaching time is in the intersection of multiple signals with different bleaching characteristics, eventually providing greater confidence in the final result. For future applications, one might consider using fewer (or even a single) pIRIR signal at the expense of less certain knowledge of the bleaching history. Furthermore, the more recent study by Cheng et al. (2022) has demonstrated that the individual grains from the same sample are subject to significant variation in the bleachability, which may result in different residual doses for different grains. The exploration on single grain scale might provide further insight into the pre-burial light exposure history of sediment.

Conclusion

Our results demonstrate that there are non-bleachable components in the IR (and possibly pIRIR) signals, and that the level of this unbleachable signal positively correlates with the preheat/stimulation temperature. It's noteworthy that the relative residual signal level is consistent between the IR_{50} and pIRIR signals for a same preheat temperature. It provides further support that lower temperature pIRIR are advantageous in reducing the contribution of residual signals (possibly induced by thermal transfer), especially when dating young samples and sediments from difficult-to-bleach environments. Taking advantage of results from our extensive bleaching experiments, we explore the pre-deposition bleaching (or transportation) history of the target sediments, based on

observation that feldspar pIRIR signals obtained at different temperatures have different bleaching characteristics. Despite the challenges, limitations, and uncertainties in this approach, we were able to quantify the possible pre-depositional sunlight bleaching time for a loess sample under investigation. That pre-depositional time amounted to an equivalent of at least 264 h exposure in the solar simulator. Our attempt provides further proof-of-concept for the utilization of luminescence dating for photochronometry (Guralnik and Sohbati, 2019), which should particularly benefit the research of sedimentological processes and provenance.

Data availability statement

The original contributions presented in the study are included in the article/Supplementary Material, further inquiries can be directed to the corresponding author.

Author contributions

JZ, ST, and BG contributed to conception and design of the study. JZ organized the database. BG performed the statistical analysis. JZ wrote the first draft of the manuscript. BG and CA rewrote part of the manuscript. All authors contributed to manuscript revision, read, and approved the submitted version.

Conflict of interest

The authors declare that the research was conducted in the absence of any commercial or financial relationships that could be construed as a potential conflict of interest.

Publisher's note

All claims expressed in this article are solely those of the authors and do not necessarily represent those of their affiliated organizations, or those of the publisher, the editors and the reviewers. Any product that may be evaluated in this article, or claim that may be made by its manufacturer, is not guaranteed or endorsed by the publisher.

Supplementary material

The Supplementary Material for this article can be found online at: https://www.frontiersin.org/articles/10.3389/feart.2022.933131/full#supplementary-material

References

Bevington, P. R., and Robinson, D. K. (2013). *Data reduction and error analysis for the physical sciences*. third ed. New York: McGraw-Hill.

Buylaert, J.-P., Jain, M., Murray, A. S., Thomsen, K. J., Thiel, C., and Sohbati, R. (2012). A robust feldspar luminescence dating method for Middle and Late Pleistocene sediments. *Boreas* 41, 435–451. doi:10.1111/j.1502-3885.2012.00248.x

Buylaert, J.-P., Murray, A. S., Gebhardt, A. C., Sohbati, R., Ohlendorf, C., Thiel, C., et al. (2013). Luminescence dating of the PASADO core 5022-1D from Laguna Potrok Aike (Argentina) using IRSL signals from feldspar. *Quat. Sci. Rev.* 71, 70–80. doi:10.1016/j.quascirev.2013.03.018

Buylaert, J. P., Murray, A. S., Thomsen, K. J., and Jain, M. (2009). Testing the potential of an elevated temperature IRSL signal from K-feldspar. *Radiat. Meas.* 44, 560–565. doi:10.1016/j.radmeas.2009.02.007

Buylaert, J. P., Thiel, C., Murray, A. S., Vandenberghe, D., Yi, S. W., and Lu, H. Y. (2011). IRSL and post IR-IRSL residual doses recorded in modern dust samples from the Chinese loess plateau. *Geochronometria* 38, 432–440. doi:10.2478/s13386-011-0047-0

Cheng, T., Zhang, D. J., Zhao, H., Yang, S. L., and Li, B. (2022). Bleachability of pIRIR signal from single-grain K-feldspar. *Quat. Geochronol.* 71, 101321. doi:10.1016/j.quageo.2022.101321

Colarossi, D., Duller, G. A. T., Roberts, H. M., Tooth, S., and Lyons, R. (2015). Comparison of paired quartz OSL and feldspar post-IR IRSL dose distributions in poorly bleached fluvial sediments from South Africa. *Quat. Geochronol.* 30, 233–238. doi:10.1016/j.quageo.2015.02.015

Dietze, M., Kreutzer, S., Fuchs, M. C., Burow, C., Fischer, M., and Schmidt, C. (2013). A practical guide to the R package luminescence. *Anc. TL* 31, 11–18.

Dr Honle Sol Sun simulation systems from Uvalight Technology Ltd (1988). *Pigment and resin Technology* (Bingley, United Kingdom: MCB UP Ltd), 17, 6. doi:10.1108/eb042547

Fu, X., Li, B., and Li, S. H. (2012). Testing a multi-step post-IR IRSL dating method using polymineral fine grains from Chinese loess. *Quat. Geochronol.* 10, 8–15. doi:10.1016/j.quageo.2011.12.004

Fu, X., and Li, S. H. (2013). A modified multi-elevated-temperature post-IR IRSL protocol for dating Holocene sediments using K-feldspar. *Quat. Geochronol.* 17, 44–54. doi:10.1016/j.quageo.2013.02.004

Guralnik, B., and Sohbati, R. (2019). "Fundamentals of photo- and thermochronometry," in *Advances in thermoluminescence and optically stimulated luminescence: Theory, experiments and applications*. Editors R. Chen and V. Pagonis (Singapore: World Scientific).

Huntley, D. J., and Lamothe, M. (2001). Ubiquity of anomalous fading in K-feldspars and the measurement and correction for it in optical dating. *Can. J. Earth Sci.* 38, 1093–1106. doi:10.1139/e01-013

Jain, M., Guralnik, B., and Andersen, M. T. (2012). Stimulated luminescence emission from localized recombination in randomly distributed defects. *J. Phys. Condens. Matter* 24, 385402–402. doi:10.1088/0953-8984/24/38/385402

Kars, R. H., Reimann, T., Ankjærgaard, C., and Wallinga, J. (2014a). Bleaching of the post-IR IRSL signal: New insights for feldspar luminescence dating. *Boreas* 43, 780–791. doi:10.1111/bor.12082

Kars, R. H., Reimann, T., and Wallinga, J. (2014b). Are feldspar SAR protocols appropriate for post-IR IRSL dating? *Quat. Geochronol.* 22, 126–136. doi:10.1016/j.quageo.2014.04.001

Li, B., Jacobs, Z., Roberts, R. G., and Li, S.-H. (2014). Review and assessment of the potential of post-IR IRSL dating methods to circumvent the problem of anomalous fading in feldspar luminescence. *Geochronometria* 41, 178–201. doi:10.2478/s13386-013-0160-3

Li, B., and Li, S. H. (2011). Luminescence dating of K-feldspar from sediments: A protocol without anomalous fading correction. *Quat. Geochronol.* 6, 468–479. doi:10.1016/j.quageo.2011.05.001

Lowick, S. E., Trauerstein, M., and Preusser, F. (2012). Testing the application of post IR- IRSL dating to fine grain waterlain sediments. *Quat. Geochronol.* 8, 33–40. doi:10.1016/j.quageo.2011.12.003

Madsen, A. T., Buylaert, J. P., and Murray, A. S. (2011). Luminescence dating of young coastal deposits from New Zealand using feldspar. *Geochronometria* 38, 379–390. doi:10.2478/s13386-011-0042-5

Murray, A. S., Thomsen, K. J., Masuda, N., Buylaert, J. P., and Jain, M. (2012). Identifying well-bleached quartz using the different bleaching rates of quartz and feldspar luminescence signals. *Radiat. Meas.* 47, 688–695. doi:10.1016/j.radmeas.2012.05.006

Nottebaum, V., Stauch, G., Kai, H., Zhang, J. R., and Lehmkuhl, F. (2015). Unmixed loess grain size populations along the northern Qilian Shan (China): Relationships between geomorphologic, sedimentologic and climatic controls. *Quat. Int.* 372, 151–166. doi:10.1016/j.quaint.2014.12.071

Ollerhead, J., and Huntley, D. J. (2011). Optical dating of young feldspars: The zeroing questions. *Anc. TL* 29, 59–63.

Reimann, T., Notenboom, P. D., De Schipper, M. A., and Wallinga, J. (2015). Testing for sufficient signal resetting during sediment transport using a polymineral multiple-signal luminescence approach. *Quat. Geochronol.* 25, 26–36. doi:10.1016/j.quageo.2014.09.002

Reimann, T., Thomsen, K. J., Jain, M., Murray, A. S., and Frechen, M. (2012). Single-grain dating of young sediments using the pIRIR signal from feldspar. *Quat. Geochronol.* 11, 28–41. doi:10.1016/j.quageo.2012.04.016

Reimann, T., and Tsukamoto, S. (2012). Dating the recent past (<500 years) by post-IR IRSL feldspar- examples from the North Sea and Baltic Sea coast. *Quat. Geochronol.* 10, 180–187. doi:10.1016/j.quageo.2012.04.011

Reimann, T., Tsukamoto, S., Naumann, M., and Frechen, M. (2011). The potential of using K-rich feldspars for optical dating of young coastal sediments – a test case from Darss-Zingst peninsula (southern Baltic Sea coast). *Quat. Geochronol.* 6, 207–222. doi:10.1016/j.quageo.2010.10.001

Rhodes, E. J. (2011). Optically stimulated luminescence dating of sediments over the past 200, 000 years. *Annu. Rev. Earth Planet. Sci.* 39, 461–488. doi:10.1146/annurev-earth-040610-133425

Sohbati, R. (2013). "Luminescence, rock surfaces," in *Encyclopedia of scientific dating methods*. Editors W. J. Rink and J. Thompson (Berlin, Germany: Springer), 7.

Sohbati, R., Murray, A. S., Buylaert, J. P., Ortuño, M., Cunha, P. P., and Masana, E. (2012). Luminescence dating of Pleistocene alluvial sediments affected by the Alhama de Murcia fault (eastern Betics, Spain) - a comparison between OSL, IRSL and post-IR IRSL ages. *Boreas* 41, 250–262. doi:10.1111/j.1502-3885.2011.00230.x

Thiel, C., Buylaert, J. P., Murray, A., Terhorst, B., Hofer, I., Tsukamoto, S., et al. (2011). Luminescence dating of the Stratzing loess profile (Austria)-Testing the potential of an elevated temperature post-IR IRSL protocol. *Quat. Int.* 234, 23–31. doi:10.1016/j.quaint.2010.05.018

Thomsen, K. J., Murray, A. S., Jain, M., and Bøtter-Jensen, L. (2008). Laboratory fading rates of various luminescence signals from feldspar-rich sediment extracts. *Radiat. Meas.* 43, 1474–1486. doi:10.1016/j.radmeas.2008.06.002

Tsukamoto, S., Kondo, R., Lauer, T., and Jain, M. (2017). Pulsed IRSL: A stable and fast bleaching luminescence signal from feldspar for dating Quaternary sediments. *Quat. Geochronol.* 41, 26–36. doi:10.1016/j.quageo.2017.05.004

Yi, S. W., Buylaert, J. P., Murray, A. S., Lu, H. Y., Thiel, C., and Zeng, L. (2016). A detailed post-IR IRSL dating study of the Niuyangzigou loess site in northeastern China. *Boreas* 45, 644–657. doi:10.1111/bor.12185

Yi, S. W., Li, X. S., Han, Z. Y., Lu, H. Y., Liu, J. F., and Wu, J. (2018). High resolution luminescence chronology for Xiashu Loess deposits of Southeastern China. *J. Asian Earth Sci.* 155, 188–197. doi:10.1016/j.jseaes.2017.11.027

Zhang, J. R., Nottebaum, V., Tsukamoto, S., Lehmkuhl, F., and Frechen, M. (2015b). Late Pleistocene and Holocene loess sedimentation in central and Western Qilian Shan (China) revealed by OSL dating. *Quat. Int.* 372, 120–129. doi:10.1016/j.quaint.2014.12.054

Zhang, J. R., Tsukamoto, S., Nottebaum, V., Lehmhuhl, F., and Frechen, M. (2015a). D$_e$ plateau and its implications for post-IR IRSL dating of polymineral fine grains. *Quat. Geochronol.* 30, 147–153. doi:10.1016/j.quageo.2015.02.003